Wind and Structures, *Vol. 25, No. 4 (2017) 329-342*
DOI: https://doi.org/10.12989/was.2017.25.4.329

An analytical solution for bending and vibration responses of functionally graded beams with porosities

Nafissa Zouatnia[1], Lazreg Hadji*[2,3] and Amar Kassoul[1]

[1]*Department of Civil Engineering, Laboratory of Structures, Geotechnics and Risks (LSGR), Hassiba Benbouali University of Chlef, Algeria, BP 151, Hay Essalam, UHB Chlef, Chlef (02000), Algeria*
[2]*Département of Civil Engineering, Ibn Khaldoun University, BP 78 Zaaroura, Tiaret (14000), Algeria*
[3]*Laboratory of Geomatics and Sustainable Development, Ibn Khaldoun University of Tiaret, Algeria*

(Received June 9, 2017, Revised September 15, 2017, Accepted September 18, 2017)

Abstract. This work presents a static and free vibration analysis of functionally graded metal–ceramic (FG) beams with considering porosities that may possibly occur inside the functionally graded materials (FGMs) during their fabrication. A new displacement field containing integrals is proposed which involves only three variables. Based on the suggested theory, the equations of motion are derived from Hamilton's principle. This theory involves only three unknown functions and accounts for parabolic distribution of transverse shear stress. In addition, the transverse shear stresses are vanished at the top and bottom surfaces of the beam. The Navier solution technique is adopted to derive analytical solutions for simply supported beams. The accuracy and effectiveness of proposed model are verified by comparison with previous research. A detailed numerical study is carried out to examine the influence of the deflections, stresses and natural frequencies on the bending and free vibration responses of functionally graded beams.

Keywords: bending, Free vibration; Functionally graded materials; integral; Hamilton's principle

1. Introduction

Functionally graded materials (FGMs) have many advantages for use in engineering structural components. Unlike fiber-matrix laminated composites, FGMs do not have problems of de-bonding and delaminating that result from large inter-laminar stresses. The concept of FGMs was initially introduced in the mid-1980s by Japanese scientists. FGMs are microscopically inhomogeneous and spatial composite materials which are usually composed of two different materials such as a pair of ceramic-metal or ceramic-polymer. The composition of the material changes gradually throughout the thickness direction. As a result, mechanical properties are assumed to vary continuously and smoothly from the top surface to the bottom. Due to good characteristics of ceramics in heat and corrosive resistances combined with the toughness of metals or high elastic of polymers, the combination of ceramics and metals or polymers can lead to excellent materials. The FGMs are widely used in mechanical, aerospace, nuclear, and civil engineering. Consequently, studies devoted to understand the static and dynamic behaviors of FGM beams and plates have being paid more and more attentions in recent years. Tai *et al.* (2011)

*Corresponding author, Dr., E-mail: had_laz@yahoo.fr

http://www.techno-press.org/?journal=was&subpage=7 ISSN: 1226-6116 (Print), 1598-6225 (Online)

used levy-type solution for buckling analysis of orthotropic plates based on two variable refined plate theory. Farahani *et al.* (2015) investigated the vibration of sumberged functionally graded cylindrical shell based on first order shear deformation theory using wave propagation method. Al-Basyouni *et al.* (2015) investigated size dependent bending and vibration analysis of functionally graded micro beams based on modified couple stress theory and neutral surface position. Benferhat *et al.* (2016a) studied the effect porosities on Static analysis of the FGM plate. Benferhat *et al.* (2016b) studied the effect of porosity on the bending and free vibration response of functionally graded plates resting on Winkler-Pasternak foundations. Ait Yahia *et al.* (2015) studied the wave propagation in functionally graded plates with porosities using various higher-order shear deformation plate theories. Bellifa *et al.* (2016) analyze the bending and free vibration analysis of functionally graded plates using a simple shear deformation theory and the concept the neutral surface position. Bounouara *et al.* (2016) used a nonlocal zeroth-order shear deformation theory for free vibration of functionally graded nanoscale plates resting on elastic foundation. Ahouel *et al.* (2016) investigated a size-dependent mechanical behavior of functionally graded trigonometric shear deformable nanobeams including neutral surface position concept. Zemri *et al.* (2015) studied a mechanical response of functionally graded nanoscale beam: an assessment of a refined nonlocal shear deformation theory beam theory. Nedri *et al.* (2014) analyze the free vibration analysis of laminated composite plates resting on elastic foundations by using a refined hyperbolic shear deformation theory. Ait Amar Meziane *et al.* (2014) proposed an efficient and simple refined theory for buckling and free vibration of exponentially graded sandwich plates under various boundary conditions. Tlidji *et al.* (2014) using the elasticity solution for bending response of functionally graded sandwich plates under thermomechanical loading. Hadji *et al.* (2014) studied the static and free vibration of FGM beam using a higher order shear deformation theory. Bourada *et al.* (2015) used a new simple shear and normal deformations theory for functionally graded beams. Mahi *et al.* (2015) investigated a new hyperbolic shear deformation theory for bending and free vibration analysis of isotropic, functionally graded, sandwich and laminated composite plates. Belabed *et al.* (2014) used an efficient and simple higher order shear and normal deformation theory for functionally graded material (FGM) plates. Bennai *et al.* (2015) used a new higher-order shear and normal deformation theory for functionally graded sandwich beams. Recently Tai *et al.* (2014) used levy Solution for free vibration analysis of functionally graded plates based on a refined plate theory. Hadji *et al.* (2015) studied the influence of the porosities on the free vibration of FGM beams. Ait Atmane *et al.* (2015) used a computational shear displacement model for Vibrational analysis of functionally graded beams with porosities.

Mouaici *et al.* (2016) studied the effect of porosity on vibrational characteristics of non-homogeneous plates using hyperbolic shear deformation theory.

This work aims to develop a new simple higher order shear deformation theory for the bending and free vibration analyses of FG beams with considering porosities that may possibly occur inside the functionally graded materials (FGMs) during their fabrication. The proposed theory has only three unknowns and three governing equations, but it satisfies the stress free boundary conditions on the top and bottom surfaces of the beam without requiring any shear correction factors. Analytical solutions are obtained for FG beam and its accuracy is verified by comparing the obtained results with those reported in the literature. The effects of various variables, such as span-to-depth ratio, gradient index and the volume fraction of porosity on bending and free vibration of FG beam are all discussed.

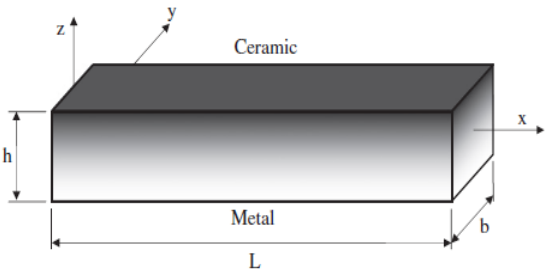

Fig. 1 Geometry and coordinate of a FG beam

2. Problem formulation

Consider a functionally graded beam with length L and rectangular cross section $\mathrm{b}\times\mathrm{h}$, with b being the width and h being the height as shown in Fig. 1. The beam is made of isotropic material with material properties varying smoothly in the thickness direction.

2.1 Effective material properties of metal ceramic functionally graded beams

The properties of FGM vary continuously due to the gradually changing volume fraction of the constituent materials (ceramic and metal), usually in the thickness direction only. The power-law function is commonly used to describe these variations of materials properties. The expression given below represents the profile for the volume fraction.

A FG beam made from a mixture of two material phases, for example, a metal and a ceramic. The material properties of FG beams are assumed to vary continuously through the thickness of the beam. In this investigation, the imperfect beam is assumed to have porosities spreading within the thickness due to defect during production. Consider an imperfect FGM with a porosity volume fraction, $\alpha(\alpha \prec\prec 1)$, distributed evenly among the metal and ceramic, the modified rule of mixture proposed by Wattanasakulpong and Ungbhakorn (2014) is used as

$$P = P_m\left(V_m - \frac{\alpha}{2}\right) + P_c\left(V_c - \frac{\alpha}{2}\right) \tag{1}$$

Now, the total volume fraction of the metal and ceramic is : $V_m + V_c = 1$, and the power law of volume fraction of the ceramic is described as

$$V_c = \left(\frac{z}{h} + \frac{1}{2}\right)^k \tag{2}$$

Hence, all properties of the imperfect FGM can be written as

$$P = \left(P_c - P_m\right)\left(\frac{z}{h} + \frac{1}{2}\right)^k + P_m - \left(P_c + P_m\right)\frac{\alpha}{2} \tag{3}$$

It is noted that the positive real number $k\ \left(0 \le k \le \infty\right)$ is the power law or volume fraction

index, and z is the distance from the mid-plane of the FG plate. The FG beam becomes a fully ceramic plate when k is set to zero and fully metal for large value of k.

Thus, the Young's modulus (E) and material density (ρ) equations of the imperfect FGM beam can be expressed as

$$E(z) = (E_c - E_m)\left(\frac{z}{h} + \frac{1}{2}\right)^k + E_m - (E_c + E_m)\frac{\alpha}{2} \tag{4}$$

$$\rho(z) = (\rho_c - \rho_m)\left(\frac{z}{h} + \frac{1}{2}\right)^k + \rho_m - (\rho_c + \rho_m)\frac{\alpha}{2} \tag{5}$$

However, Poisson's ratio (ν) is assumed to be constant. The material properties of a perfect FG beam can be obtained when α is set to zero.

2.2 Kinematics and constitutive equations

The displacement field can be obtained

$$u(x,z,t) = u_0(x,t) - z\frac{\partial w_0}{\partial x} + k_1\, f(z)\int \theta(x,t)\,dx \tag{6a}$$

$$w(x,z,t) = w_0(x,t) \tag{6b}$$

In this work, the present higher-order shear deformation beam theory is obtained by setting

$$f(z) = \frac{1}{2}z\left(\frac{1}{4}h^2 - \frac{1}{3}z^2\right) \tag{7}$$

The strains associated with the displacements in Eq. (6) are

$$\varepsilon_x = \varepsilon_x^0 + z\,k_x^b + f(z)\,k_x^s \tag{8a}$$

$$\gamma_{xz} = g(z)\,\gamma_{xz}^0 \tag{8b}$$

where

$$\varepsilon_x^0 = \frac{\partial u_0}{\partial x},\ k_x^b = -\frac{\partial^2 w_b}{\partial x^2},\ k_x^s = k_1\theta,\ \gamma_{xz}^0 = k_1\int \theta\,dx \tag{8c}$$

and

$$g(z) = \frac{df(z)}{dz} \tag{8d}$$

The integral defined in the above equations shall be resolved by a Navier type method and can be written as follow:

$$\int \theta \, dx = A' \frac{\partial \theta}{\partial x} \tag{9}$$

where the coefficient A' is expressed according to the type of solution used, in this case via Navier. Therefore, A' and k_1 are expressed as follows

$$A' = -\frac{1}{\alpha^2}, \quad k_1 = \alpha^2 \tag{10}$$

where α is defined in expression (22).

The state of stress in the beam is given by the generalized Hooke's law as follows

$$\sigma_x = Q_{11}(z)\,\varepsilon_x \quad \text{and} \quad \tau_{xz} = Q_{55}(z)\,\gamma_{xz} \tag{11a}$$

where

$$Q_{11}(z) = E(z) \quad \text{and} \quad Q_{55}(z) = \frac{E(z)}{2(1+\nu)} \tag{11b}$$

2.3 Equations of motion

Hamilton's principle is used herein to derive the equations of motion. The principle can be stated in analytical form as (Thai and Vo 2012)

$$\delta \int_{t_1}^{t_2} (U + V - T) dt = 0 \tag{12}$$

where t is the time; t_1 and t_2 are the initial and end time, respectively; δU is the virtual variation of the strain energy; δV is the virtual variation of the potential energy; and δT is the virtual variation of the kinetic energy. The variation of the strain energy of the beam can be stated as

$$\begin{aligned} \delta U &= \int_0^L \int_{-\frac{h}{2}}^{\frac{h}{2}} (\sigma_x \delta \varepsilon_x + \tau_{xz} \delta \gamma_{xz}) dz dx \\ &= \int_0^L \left(N \frac{d\delta u_0}{dx} - M_b \frac{d^2 \delta w_b}{dx^2} - M_s \frac{d^2 \delta w_s}{dx^2} + Q \frac{d\delta w_s}{dx} \right) dx \end{aligned} \tag{13}$$

where N, M_b, M_s and Q are the stress resultants defined as

$$(N, M_b, M_s) = \int_{-\frac{h}{2}}^{\frac{h}{2}} (1, z, f)\, \sigma_x dz \quad \text{and} \quad Q = \int_{-\frac{h}{2}}^{\frac{h}{2}} g\, \tau_{xz} dz \tag{14}$$

The variation of the potential energy by the applied transverse load q can be written as

$$\delta V = -\int_0^L q\delta w_0 dx \tag{15}$$

The variation of the kinetic energy can be expressed as

$$\begin{aligned}\delta T &= \int_0^L \int_{-\frac{h}{2}}^{\frac{h}{2}} \rho(z)\left[\dot{u}\delta\dot{u} + \dot{w}\delta\dot{w}\right]dzdx \\ &= \int_0^L \left\{ I_0\left[\dot{u}_0\delta\dot{u}_0 + \dot{w}_0\delta\dot{w}_0\right] - I_1\left(\dot{u}_0\frac{\partial\delta\dot{w}_0}{\partial x} + \frac{\partial\dot{w}_0}{\partial x}\delta\dot{u}_0\right)\right. \\ &\quad + J_1\left(\left(k_1A'\right)\left(\dot{u}_0\frac{\partial\delta\dot{\theta}}{\partial x} + \frac{d\dot{\theta}}{\partial x}\delta\dot{u}_0\right)\right) + I_2\left(\frac{\partial\dot{w}_0}{\partial x}\frac{\partial\delta\dot{w}_0}{\partial x}\right) \\ &\quad \left. + K_2\left(k_1A'\right)^2\left(\frac{d\dot{\theta}}{\partial x}\frac{\partial\delta\dot{\theta}}{\partial x}\right) - J_2\left(\left(k_1A'\right)\left(\frac{\partial\dot{w}_0}{\partial x}\frac{\partial\delta\dot{\theta}}{\partial x} + \frac{\partial\dot{\theta}}{\partial x}\frac{\partial\delta\dot{w}_0}{\partial x}\right)\right)\right\}dx\end{aligned} \tag{16}$$

where dot-superscript convention indicates the differentiation with respect to the time variable t; $\rho(z)$ is the mass density; and (I_i, J_i, K_i) are mass inertias expressed by

$$\left(I_0, I_1, I_2\right) = \int_{-h/2}^{h/2}\left(1, z, z^2\right)\rho(z)dz \tag{17a}$$

$$\left(J_1, J_2, K_2\right) = \int_{-h/2}^{h/2}\left(f, z\ f, f^2\right)\rho(z)dz \tag{17b}$$

By substituting Eqs. (13), (15) and (16) into Eq. (12), the following can be derived:

$$\delta u_0 : \ \frac{dN}{dx} = I_0\ddot{u}_0 - I_1\frac{\partial\ddot{w}_0}{\partial x} + k_1A'J_1\frac{\partial\ddot{\theta}}{\partial x} \tag{18a}$$

$$\delta w_0 : \frac{d^2M_b}{dx^2} + q = I_0\ddot{w}_0 + I_1\frac{\partial\ddot{u}_0}{\partial x} - I_2\frac{\partial^2\ddot{w}_0}{\partial x^2} + J_2k_1A'\frac{\partial^2\ddot{\theta}}{\partial x^2} \tag{18b}$$

$$\delta\theta : -\mathrm{k}_1M_x^s + k_1A'\frac{\partial Q}{\partial x} = -J_1k_1A'\frac{\partial\ddot{u}_0}{\partial x} - K_2\left(k_1A'\right)^2\frac{\partial^2\ddot{\theta}}{\partial x^2} + J_2k_1A'\frac{\partial^2\ddot{w}_0}{\partial x^2} \tag{18c}$$

Introducing Eq. (14) into Eq. (18), the equations of motion can be expressed in terms of displacements (u_0, w_0, θ) and the appropriate equations take the form

$$A_{11}\frac{\partial^2 u_0}{\partial x^2} - B_{11}\frac{\partial^3 w_0}{\partial x^3} + B_{11}^s k_1 \frac{\partial \theta}{\partial x} = I_0 \ddot{u}_0 - I_1 \frac{\partial \ddot{w}_0}{\partial x} + J_1 A' k_1 \frac{\partial \ddot{\theta}}{\partial x} \tag{19a}$$

$$B_{11}\frac{\partial^3 u_0}{\partial x^3} - D_{11}\frac{\partial^4 w_0}{\partial x^4} + D_{11}^s k_1 \frac{\partial^2 \theta}{\partial x^2} + q = I_0 \ddot{w}_0 + I_1 \frac{\partial \ddot{u}_0}{\partial x} - I_2 \frac{\partial^2 \ddot{w}_0}{\partial x^2} + J_2 k_1 A' \frac{\partial^2 \ddot{\theta}}{\partial x^2} \tag{19b}$$

$$-B_{11}^s k_1 \frac{\partial u_0}{\partial x} + D_{11}^s k_1 \frac{\partial^2 w_0}{\partial x^2} - H_{11}^s k_1^2 \theta + A_{55}^s (k_1 A')^2 \frac{\partial^2 \theta}{\partial x^2} = -J_1 k_1 A' \frac{\partial \ddot{u}}{\partial x} + J_2 k_1 A' \frac{\partial^2 \ddot{w}_0}{\partial x^2} - K_2 (k_1 A')^2 \frac{\partial^2 \ddot{\theta}}{\partial x^2} \tag{19c}$$

where A_{11}, D_{11}, etc., are the beam stiffness, defined by

$$\left(A_{11}, B_{11}, D_{11}, B_{11}^s, D_{11}^s, H_{11}^s\right) = \int_{-\frac{h}{2}}^{\frac{h}{2}} Q_{11}\left(1, z, z^2, f(z), z\, f(z), f^2(z)\right) dz \tag{20a}$$

and

$$A_{55}^s = \int_{-\frac{h}{2}}^{\frac{h}{2}} Q_{55}\left[g(z)\right]^2 dz \tag{20b}$$

3. Analytical solution

The equations of motion admit the Navier solutions for simply supported beams. The variables u_0, w_0, θ can be written by assuming the following variations

$$\begin{Bmatrix} u_0 \\ w_0 \\ \theta \end{Bmatrix} = \sum_{m=1}^{\infty} \begin{Bmatrix} U_m \cos(\alpha x) e^{i\omega t} \\ W_m \sin(\alpha x) e^{i\omega t} \\ X_m \sin(\alpha x) e^{i\omega t} \end{Bmatrix} \tag{21}$$

where ω is the frequency of free vibration of the plate, $\sqrt{i} = -1$ the imaginary unit. with

$$\alpha = m\pi / L \tag{22}$$

The transverse load q is also expanded in Fourier series as

$$q(x) = \sum_{m=1}^{\infty} Q_m \sin(\alpha x) \tag{23a}$$

where Q_m is the load amplitude calculated from

$$Q_m = \frac{2}{L}\int_0^L q(x)\sin(\alpha\, x)dx \tag{23b}$$

Substituting Eqs. (21) and (23) into Eq. (19), the following problem is obtained

$$\left(\begin{bmatrix} S_{11} & S_{12} & S_{13} \\ S_{12} & S_{22} & S_{23} \\ S_{13} & S_{23} & S_{33} \end{bmatrix} - \omega^2 \begin{bmatrix} m_{11} & m_{12} & m_{13} \\ m_{12} & m_{22} & m_{23} \\ m_{13} & m_{23} & m_{33} \end{bmatrix}\right)\begin{Bmatrix} U_m \\ W_m \\ X_m \end{Bmatrix} = \begin{Bmatrix} 0 \\ Q_m \\ 0 \end{Bmatrix} \tag{24}$$

where

$$S_{11} = A_{11}\alpha^2,\ S_{12} = -B_{11}\alpha^3,\ S_{13} = -B_{11}^s\alpha k_1,$$

$$S_{22} = D_{11}\alpha^4,\ S_{23} = D_{11}^s\alpha^2 k_1,\quad S_{33} = H_{11}^s k_1^2 + A_{55}^s\left(k_1 A'\right)^2\alpha^2$$

$$m_{11} = I_0,\ m_{12} = -I_1\alpha,\ m_{13} = J_1\alpha k_1 A',$$

$$m_{22} = I_0 + I_2\alpha^2,\ m_{23} = -J_2\alpha^2 k_1\, A',$$

$$m_{33} = K_2\alpha^2\left(k_1\, A'\right)^2 \tag{25}$$

4. Results and discussion

In this section, various numerical examples are presented and discussed to verify the accuracy of the present theory in predicting the bending and free vibration of simply supported FG beams. The FG beam is taken to be made of aluminum and alumina with the following material properties:

Ceramic (P_C : Alumina, Al_2O_3): $E_c = 380$ GPa; $\nu = 0.3$; $\rho_c = 3960$ kg/m^3.

Metal (P_M : Aluminium, Al): $E_m = 70$ GPa; $\nu = 0.3$; $\rho_m = 2702$ kg/m^3.

And their properties change through the thickness of the beam according to power-law. The bottom surfaces of the FG beams are aluminum rich, whereas the top surfaces of the FG beams are alumina rich.

For convenience, the following dimensionless form is used:

$$\bar{w} = 100\frac{E_m h^3}{q_0 L^4} w\left(\frac{L}{2}\right),\quad \bar{u} = 100\frac{E_m h^3}{q_0 L^4} u\left(0,-\frac{h}{2}\right),\quad \bar{\sigma}_x = \frac{h}{q_0 L}\sigma_x\left(\frac{L}{2},\frac{h}{2}\right),\quad \bar{\tau}_{xz} = \frac{h}{q_0 L}\tau_{xz}(0,0)$$

$$\bar{\omega} = \frac{\omega L^2}{h}\sqrt{\frac{\rho_m}{E_m}}$$

4.1 Results for bending analysis

Table 1 contains nondimensional deflection and stresses of perfect and imperfect FG beams under uniform load for different values of power law index and span-to-depth ratio. The obtained results are compared with various shear deformation beam theories (i.e., ESDBT, SSDBT, PSDBT) and Le *et al*. (2010). It can be observed that the values obtained using various shear deformation beam theories (i.e., ESDBT, SSDBT, PSDBT) and Le are in good agreement with the those given by the present theory for perfect FG beams and for all values of power law index p and span-to-depth ratio L/h and takes maximum values for the imperfect FG beam ($\alpha = 0.1$ and $\alpha = 0.2$). This is expected because the imperfect FG beam is the one with the lowest stiffness and the perfect FG beam is the one with the highest stiffness. In addition the comparisons show that the effect of the porosity on the deflection of FG beams. The results reveal that the deflection results increase as the volume fraction of porosity (α) increases. Due to ignoring the shear deformation effect, CBT underestimates deflection of moderately deep beams.

Figs. 2 show the variations of axial stress $\bar{\sigma}_x$, through the depth of the perfect and imperfect FG baem for $p = 1$ under uniform load. The stresses are tensile at the top surface and compressive at the bottom surface and take the maximum values for the imperfect FG beam. Figs. 3, shows the distribution of the shear stresses $\bar{\tau}_{xz}$ through the thickness of the FG beam. The volume fraction exponent of the FG beam in taken as $p = 1$. It's clear that the distributions are not parabolic and the stresses increase for the imperfect FG beam.

Fig. 4 illustrates the variation of the non-dimensional transversal displacement of perfect and imperfect FG beams based on the present plate theory versus non-dimensional length for different power law index. The deflection is maximum for the imperfect FG beam ($\alpha = 0.1$ and $\alpha = 0.2$) and minimum for the perfect FG plate ($\alpha = 0$). In addition, the results show that the increase of the power law index leads to an increase of transversal displacement.

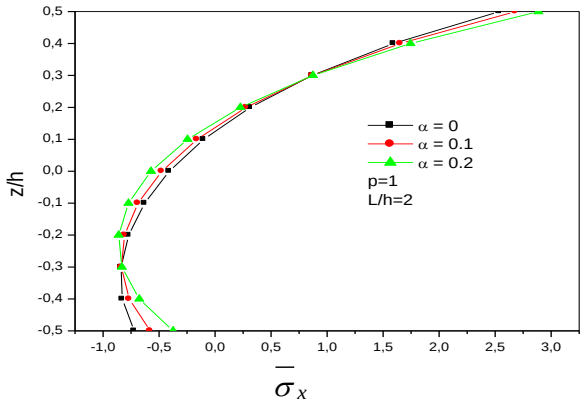

Fig. 2 Variation of nondimensional axial normal stress $\bar{\sigma}_x(l/2, z)$ across the depth of FG beams under uniform load

Table 1 Nondimensional deflections and stresses of FG beams under uniform load

k	Method		$L/h=5$				$L/h=20$			
		α	$\bar{w}$	$\bar{u}$	$\bar{\sigma}_x$	$\bar{\tau}_{xz}$	$\bar{w}$	$\bar{u}$	$\bar{\sigma}_x$	$\bar{\tau}_{xz}$
0	CBT*	$\alpha=0$	2.8783	0.9211	3.7500	-	2.8783	0.2303	15.0000	-
	PSDBT*	$\alpha=0$	3.1654	0.9398	3.8019	0.7330	2.8962	0.2306	15.0129	0.7437
	Li *et al.* (2010)	$\alpha=0$	3.1657	0.9402	3.8020	0.7500	2.8962	0.2306	15.0130	0.7500
	Present	$\alpha=0$	3.1654	0.9398	3.8019	0.7330	2.8962	0.2305	15.0128	0.7436
		$\alpha=0.1$	3.3646	0.9989	3.8019	0.7330	3.0785	0.2450	15.0128	0.7436
		$\alpha=0.2$	3.5906	1.0660	3.8018	0.7330	3.2852	0.2615	15.0128	0.7436
1	CBT*	$\alpha=0$	5.7746	2.2722	5.7958	-	5.7746	0.5680	23.1834	-
	PSDBT*	$\alpha=0$	6.2594	2.3038	5.8835	0.7330	5.8049	0.5686	23.2051	0.7437
	Li *et al.* (2010)	$\alpha=0$	6.2599	2.3045	5.8837	0.7500	5.8049	0.5686	23.2054	0.7500
	Present	$\alpha=0$	6.2594	2.3038	5.8834	0.7330	5.8049	0.5685	23.2051	0.7437
		$\alpha=0.1$	7.2507	2.7310	6.2195	0.7330	6.7457	0.6745	24.5346	0.7437
		$\alpha=0.2$	8.6774	3.3637	6.7061	0.7330	8.1093	0.8316	26.4622	0.7437
5	CBT*	$\alpha=0$	8.7508	3.6496	7.9428	-	8.7508	0.9124	31.7711	-
	PSDBT*	$\alpha=0$	9.8281	3.7100	8.1104	0.5904	8.8182	0.9134	31.8127	0.6013
	Li *et al.* (2010)	$\alpha=0$	9.7802	3.7089	8.1030	0.5790	8.8151	0.9133	31.8112	0.5790
	Present	$\alpha=0$	9.8281	3.7100	8.1104	0.5904	8.8182	0.9134	31.8127	0.6013
		$\alpha=0.1$	12.9183	5.1357	9.0711	0.5495	11.6160	1.2667	35.5387	0.5601
		$\alpha=0.2$	20.0934	8.6894	11.0613	0.4733	18.2672	2.1517	43.2983	0.4831
10	CBT*	$\alpha=0$	9.6072	3.8097	9.5228	-	9.6072	0.9524	38.0912	-
	PSDBT*	$\alpha=0$	10.9381	3.8864	9.7119	0.6465	9.6905	0.9536	38.1382	0.6586
	Li *et al.* (2010)	$\alpha=0$	10.8979	3.8860	9.7063	0.6436	9.6879	0.9536	38.1372	0.6436
	Present	$\alpha=0$	10.9381	3.8863	9.7119	0.6465	9.6905	0.9536	38.1382	0.6586
		$\alpha=0.1$	14.5261	5.4151	10.9461	0.6168	12.7847	1.3296	42.8964	0.6290
		$\alpha=0.2$	23.1357	9.4017	13.1949	0.5496	20.2308	2.3133	51.4893	0.5617

4.2 Results for free vibration analysis

Tables 2 and 3 shows the nondimensional fundamental frequencies $\bar{\omega}$ of perfect and imperfect FG beams of FG beams for different values of power law index p and span-to-depth ratio L/h. The calculated frequencies are compared with those given by Simsek. (2010) using various beam theories. An excellent agreement between the present theory and results of Simsek. (2010) is found. The results reveal that the frequency results decrease as the volume fraction of porosity (α) increases.

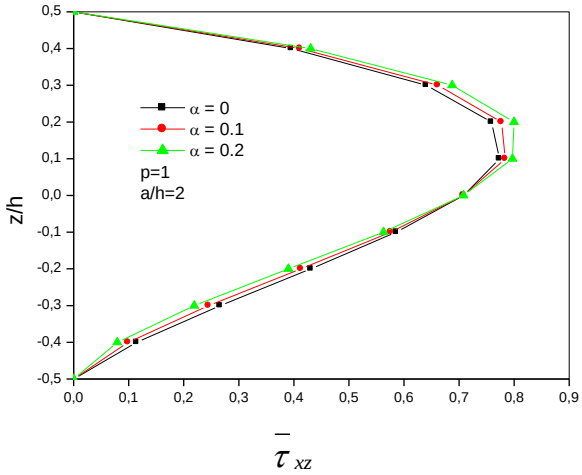

Fig. 3 Variation of nondimensional transverse shear stress $\bar{\tau}_{xz}(0,z)$ across the depth of FG beams under uniform m load

Table 2 Variation of fundamental frequency $\bar{\omega}$ with the power-law index for FG beam for $\mathrm{L/h}=5$

Theory	α	$p=0$	$p=0.2$	$p=0.5$	$p=1$	$p=5$	$p=10$	Metal
CBT*	$\alpha=0$	5.3953	5.0206	4.5931	4.1484	3.5949	3.4921	2.8034
FSDBT*	$\alpha=0$	5.1525	4.8066	4.4083	3.9902	3.4312	3.3134	2.6772
ESDBT*	$\alpha=0$	5.1542	4.8105	4.4122	3.9914	3.4014	3.2813	2.6781
PSDBT*	$\alpha=0$	5.1527	4.8092	4.4111	3.9904	3.4012	3.2816	2.6773
	$\alpha=0$	5.1527	4.8081	4.4107	3.9904	3.4012	3.2816	2.6773
Present	$\alpha=0.1$	5.2223	4.8498	4.4042	3.9070	3.1478	3.0292	2.3554
	$\alpha=0.2$	5.3048	4.8995	4.3928	3.7865	2.6961	2.5718	1.8433

* Results form Ref (Simsek 2010)

Table 3 Variation of fundamental frequency $\bar{\omega}$ with the power-law index for FG beam for $L/h=20$

Theory	α	$p=0$	$p=0.2$	$p=0.5$	$p=1$	$p=5$	$p=10$	Metal
CBT*	$\alpha=0$	5.4777	5.0967	4.6641	4.2163	3.6628	3.5546	2.8462
FSDBT*	$\alpha=0$	5.4603	5.0827	4.6514	4.2051	3.6509	3.5415	2.8371
ESDBT*	$\alpha=0$	5.4604	5.0829	4.6516	4.2051	3.6483	3.5389	2.8372
PSDBT*	$\alpha=0$	5.4603	5.0829	4.6516	4.2050	3.6485	3.5389	2.8372
	$\alpha=0$	5.4603	5.0815	4.6511	4.2050	3.6485	3.5389	2.8371
Present	$\alpha=0.1$	5.5340	5.1244	4.6412	4.1117	3.3767	3.2809	2.4960
	$\alpha=0.2$	5.6214	5.1755	4.6254	3.9776	2.8856	2.8021	1.9533

* Results form Ref (Simsek 2010)

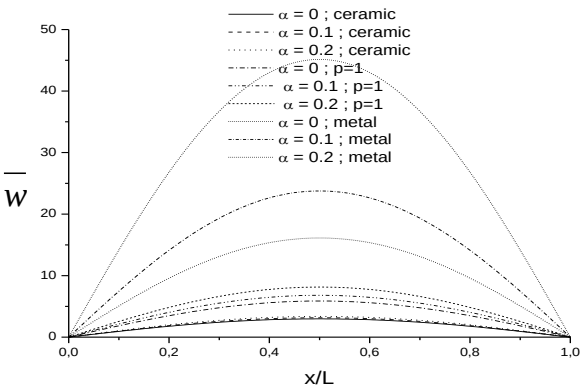

Fig. 4 Variation of the transverse displacement $\overline{w}$ versus non-dimensional length of a FG beam ($L = 5h$)

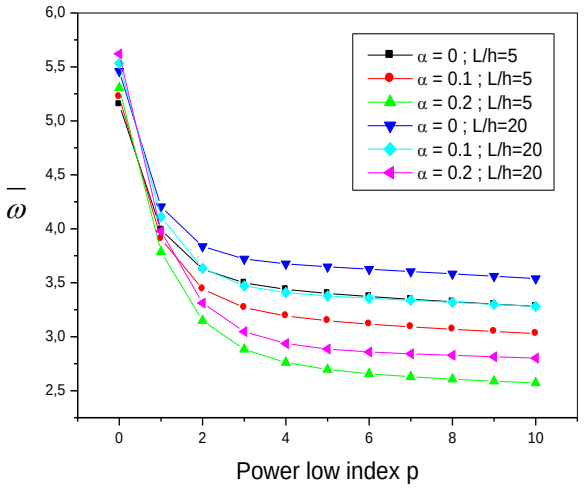

Fig. 5 Variation of the fundamental frequency $\overline{\omega}$ of FG beam with power-law index

Fig. 5 shows the non-dimensional fundamental natural frequency $\overline{\omega}$ of perfect and imperfect FG beams versus the power law index for different values of span-to-depth ratio using the present theory. It is observed that an increase in the value of the power law index p leads to a reduction of frequency. In addition, the porosity leads to a decrease of the frequency of the beam.

5. Conclusions

Bending and vibration analysis of perfect and imperfect FG beams under uniform load is carried out in the present study by a new shear deformation beam theory.

The theory inherently satisfies the condition of zero transverse shear stresses on the top and bottom surfaces of the beam. The results generated in the present work for various analyses are compared with the existing published results. The comparison proves the accuracy of the presently considered shear deformation theory, and hence it can successfully be employed for the structural analyses of FG beam.

References

Ahouel et al. (2016), "Size-dependent mechanical behavior of functionally graded trigonometric shear deformable nanobeams including neutral surface position concept", *Steel Compos. Struct.*, **20**(5), 963-981.

Ait Amar Meziane, M., Abdelaziz, H.H. and Tounsi, A. (2014), "An efficient and simple refined theory for buckling and free vibration of exponentially graded sandwich plates under various boundary conditions", *J. Sandw. Struct. Mater*., **16**(3), 293-318.

Ait Atmane, H., Tounsi, A., Bernard, F. and Mahmoud, S.R. (2015), "A computational shear displacement model for Vibrational analysis of functionally graded beams with porosities", *Steel Compos. Struct*., **19**(2), 369-385.

Ait Yahia, S., Ait Atmane, H., Houari, M.S.A. and Tounsi, A. (2015), "Wave propagation in functionally graded plates with porosities using various higher-order shear deformation plate theories", *Struct. Eng. Mech*., **53**(6), 1143-1165.

Al-Basyouni, K.S., Tounsi, A. and Mahmoud, S.R. (2015), "Size dependent bending and vibration analysis of functionally graded micro beams based on modified couple stress theory and neutral surface position", *Compos. Struct.*, **125**, 621-630.

Belabed, Z., Houari, M.S.A., Tounsi, A., Mahmoud, S.R. and Anwar Bég, O. (2014), "An efficient and simple higher order shear and normal deformation theory for functionally graded material (FGM) plates", *Compos.: Part B*, **60**, 274-283.

Bellifa, H., Benrahou, K.H., Hadji, L., Houari, M.S.A. and Tounsi, A. (2016), "Bending and free vibration analysis of functionally graded plates using a simple shear deformation theory and the concept the neutral surface position", *J. Braz. Soc. Mech. Sci. Eng*., **38**, 265-275.

Benferhat, R., Hassaine Daouadji, T., Hadji, L. and Said Mansour, M. (2016a), "Static analysis of the FGM plate with porosities", *Compos. Struct.*, **21**(1), 123-136.

Benferhat, R., Hassaine Daouadji, T., Said Mansour, M. and Hadji, L., (2016b), "Effect of porosity on the bending and free vibration response of functionally graded plates resting on Winkler-Pasternak foundations", *Earthq. Struct.*, **10**(6) , 1429-1449.

Bennai, R., Ait Atmane, H. and Tounsi, A. (2015), "A new higher-order shear and normal deformation theory for functionally graded sandwich beams", *Steel Compos. Struct.*, **19**(3), 521 -546.

Bounouara, F., Benrahou, K.H., Belkorissat, I. and Tounsi, A. (2016), "A nonlocal zeroth-order shear deformation theory for free vibration of functionally graded nanoscale plates resting on elastic foundation", *Steel and Compos. Struct*., **20**(2), 227-249.

Bourada, M., Kaci, A., Houari, M.S.A. and Tounsi, A. (2015), "A new simple shear and normal deformations theory for functionally graded beams", *Steel Compos. Struct.*, **18**(2), 409-423.

Farahani, H. and Barati, F. (2015), "Vibration of sumberged functionally graded cylindrical shell based on first order shear deformation theory using wave propagation method", *Struct. Eng. Mech*., **53**(3), 575-587.

Hadji, L., and Adda Bedia, E.A., (2015) "Influence of the porosities on the free vibration of FGM beams", *Wind Struct.*, **21**(3) 273-287.

Hadji, L., Daouadji, T.H., Tounsi, A. and Bedia, E.A. (2014), "A higher order shear deformation theory for static and free vibration of FGM beam", *Steel Compos. Struct.*, **16**(5), 507-519.

Li, X.F., Wang, B.L. and Han, J.C. (2010), "A higher-order theory for static and dynamic analyses of functionally graded beams", *Arch. Appl . Mech.*, **80**(10), 1197-1212.

Mahi, A., Adda Bedia, E.A. and Tounsi, A. (2015), "A new hyperbolic shear deformation theory for bending and free vibration analysis of isotropic, functionally graded, sandwich and laminated composite plates", *Appl. Math. Model.*, **39**, 2489-2508.

Mouaici, F., Benyoucef, S., Ait Atmane, H. and Tounsi, A, (2016), "Effect of porosity on vibrational characteristics of non-homogeneous plates using hyperbolic shear deformation theory", *Wind Struct.*, **22**(4), 429-454.

Nedri, K., El Meiche, N. and Tounsi, A. (2014), "Free vibration analysis of laminated composite plates resting on elastic foundations by using a refined hyperbolic shear deformation theory", *Mech. Compos. Mater*., **49**(6), 641-650.

Simsek, M. (2010), "Fundamental frequency analysis of functionally graded beams by using different higher-order beam theories", *Nucl. Eng. Des*., **240**(4), 697-705.

Tai, H.T. and Choi, D.H. (2014), "Levy solution for free vibration analysis of functionally graded plates based on a refined plate theory", *J. Civil. Eng.- KSCE*, **18**(6),1813-1824.

Tai, H.T. and Kim, S.E. (2011), "Levy-type solution for buckling analysis of orthotropic plates based on two variable refined plate theory", *Compos. Struct.*, **93(**7), 1738-1746.

Thai, H.T. and Vo, T.P. (2012), "Bending and free vibration of functionally graded beams using various higher-order shear deformation beam theories", *Int. J. Mech. Sci*., **62**(1), 57-66.

Tlidji, Y., Hassaine Daouadji, T., Hadji, L., Tounsi, A. and Adda Bedia, E.A. (2014), "Elasticity solution for bending response of functionally graded sandwich plates under thermomechanical loading", *J. Therm, Stresses*, **37**(7), 852-869.

Wattanasakulpong, N. and Ungbhakorn, V. (2014), "Linear and nonlinear vibration analysis of elastically restrained ends FGM beams with porosities", *Aerosp. Sci. Technol.*, **32**(1), 111-120.

Zemri, A., Houari, M.S.A., Bousahla, A.A. and Tounsi, A. (2015), "A mechanical response of functionally graded nanoscale beam: an assessment of a refined nonlocal shear deformation theory beam theory", *Struct. Eng. Mech*., **54**(4), 693-710.

CC